

000 001 002 003 004 005 006 007 008 009 010 011 012 013 014 015 016 017 018 019 020 021 022 023 024 025 026 027 028 029 030 031 032 033 034 035 036 037 038 039 040 041 042 043 044 045 046 047 048 049 050 051 052 053 ROTATION CONTROL UNLEARNING: QUANTIFYING AND CONTROLLING CONTINUOUS UNLEARNING FOR LLM WITH THE COGNITIVE ROTATION SPACE

Anonymous authors

Paper under double-blind review

ABSTRACT

As Large Language Models (LLMs) become increasingly prevalent, their security vulnerabilities have already drawn attention. Machine unlearning is introduced to seek to mitigate these risks by removing the influence of undesirable data. However, existing methods not only rely on the retained dataset to preserve model utility, but also suffer from cumulative catastrophic utility loss under continuous unlearning requests. To solve this dilemma, we propose a novel method, called Rotation Control Unlearning (RCU), which leverages the rotational salience weight of RCU to quantify and control the unlearning degree in the continuous unlearning process. The skew symmetric loss is designed to construct the existence of the cognitive rotation space, where the changes of rotational angle can simulate the continuous unlearning process. Furthermore, we design an orthogonal rotation axes regularization to enforce mutually perpendicular rotation directions for continuous unlearning requests, effectively minimizing interference and addressing cumulative catastrophic utility loss. Experiments on multiple datasets confirm that our method without retained dataset achieves SOTA performance.

1 INTRODUCTION

In recent years, the development of Large Language Models (LLMs) has received widespread attention. With the extensive application of GPT (Achiam et al. (2023)) and other LLMs (Liu et al. (2024); Touvron et al. (2023)) in academic research and industry (Wang et al. (2024)), concerns about LLMs have also increased. Among these, security issues regarding information protection have become particularly prominent. These concerns have motivated researchers to use the machine unlearning method to remove potentially private (Ortiz-Jimenez et al. (2023)), illegal or toxic data that may exist in LLMs. Currently, machine unlearning in LLMs (Bourtoule et al. (2021)) is mainly divided into two paradigms: the method based on parameters (Chen & Yang (2023b); Eldan & Russinovich (2023); Jia et al. (2024)) and the method based on in-context unlearning (Thaker et al. (2024); Pan et al. (2020)). The methods based on parameters achieve effective unlearning by maximizing the task loss on the unlearning data (Wang et al. (2025a); Hu et al. (2025)). The methods based on in-context unlearning modify the input prompts of LLM to make them refuse to output the content that needs to be unlearning (Chen et al. (2025); Yu et al. (2025)). Other methods achieve the unlearning goal by interfering with the LLM’s representation of the unlearned data (He et al. (2025); Jiang et al. (2025)).

However, unlearning methods in LLM are often not a one-time operation but a continuous process in real world. Most of them exist the cumulative catastrophic utility loss (Gao et al. (2025)) when dealing with continuous unlearning. The cumulative catastrophic utility loss causes a significant decline in both the LLM’s unlearning capability and utility retention capacity during the continuous unlearning process as the number of requests increases. At the parameter level, this manifests as new unlearning requests inducing parameter shift in previously learned ones. Furthermore, they still require a retained dataset to maintain the model’s utility. This retained dataset consists of a part of the original training dataset (Bourtoule et al. (2021)). Since LLM require a large amount of data for training (Wang et al. (2024)), using the retained dataset in continuous unlearning is not feasible (Liu et al. (2025)).

The work of o^3 (Gao et al. (2025)) proposes to mitigate cumulative catastrophic utility loss by imposing orthogonal constraints on LoRA parameters and introduces weights for the LoRA (Hu et al. (2022)) modules to represent the degree of unlearning. However, this approach suffers from several significant limitations. Firstly, the effectiveness of its simple orthogonal constraints on LoRA parameters diminishes as the number of unlearning requests increases, making it difficult to sustainably alleviate cumulative catastrophic utility loss. Secondly, using LoRA weights to quantify the degree of unlearning lacks interpretable justification. Finally, the mapping from the Out-Of-Distribution (OOD) detector outputs to the corresponding weights heavily relies on empirical design, which substantially increases the complexity and cost of application.

In this work, we propose Rotation Control Unlearning (RCU), a novel unlearning method that addresses the above challenges. This method is inspired by the theory of Lie group (Gallier (2001)) and re-constructs the LoRA update paradigm through mathematical derivation. It re-expresses the unlearning update of LLM as rotational operations within a cognitive rotation space. The cognitive rotation space is defined as a high-dimensional rotation space, which is used to depict the rotational transformations experienced by the original parameters of LLM during continuous unlearning. This enables the transformation of the uncontrollable parameter shift into controllable rotational angle changes, thereby effectively alleviating the cumulative catastrophic utility loss. The specific mathematical formulation is elaborated in the methodology. Our approach introduces a skew symmetric loss in LoRA update paradigm to formulate the unlearning process as rotation operations, with the rotational angle serving as a precise quantification metric. We introduce an orthogonal rotation axes loss to enforce perpendicular rotation directions for consecutive unlearning requests, effectively mitigating cumulative catastrophic utility loss by minimizing inter unlearning request interference. Furthermore, to enhance compatibility, we design an unlearning alignment loss that guides the OOD detector to produce representations aligned with our LoRA update paradigm. These representations then collaborate with the distributional shift compensator to generate rotational salience weights for auxiliary quantification. Finally, our method is supported by straightforward experimental interpretability and requires significantly fewer trainable parameters than o^3 .

Specifically, our contributions are outlined as follows:

- We propose the RCU method, which quantifies the unlearning process by leveraging rotational changes in the cognitive rotation space, and introduce the rotational salience weight to precisely control the degree of unlearning throughout the continuous unlearning process.
- We design the skew symmetric loss to establish the existence of the cognitive rotation space and the orthogonal rotation axes loss to alleviate cumulative catastrophic utility loss.
- We demonstrate the connection between rotation and unlearning through mathematical proof and experimental validation.
- Extensive experiments on the ScienceQA and TOFU datasets confirm the effectiveness of our proposed method without retained dataset.

2 PRELIMINARY

Machine Unlearning in LLMs. The objective of machine unlearning is to safeguard information security. Currently, there are two mainstream approaches: parameters-based methods Chen & Yang (2023b); Eldan & Russinovich (2023); Jia et al. (2024) and in-context unlearning-based methods. Thaker et al. (2024); Pan et al. (2020) Parameters-based methods iteratively adjust the LLMs' internal parameters to minimize the loss function on specific tasks, thereby improving unlearning performance (Yi et al. (2025); Yang et al. (2025); Bronec & Helcl (2025); Prempatis et al. (2025)). Yi et al. (2025) method employs fine-tuning for rapid learning and induces deliberate model degradation upon detection of harmful fine-tuning behaviors. Yang et al. (2025) approach utilizes a reweighting strategy to adjust training sample weights, focusing particularly on data useful for unlearning. In-context unlearning-based methods modify input prompts to prevent the generation of undesired content. Yu et al. (2025) method generates tokens that guide forgetting based on the input query, achieving unlearning without altering model parameters. Additionally, other techniques exist (Muhammed et al. (2025); Wang et al. (2025b)). For instance, Muhammed et al. (2025)s control forgetting by manipulating model activations. The He et al. (2025) method disrupts the latent space of forgotten samples during training to induce chaotic outputs. The Zhao et al. (2025) has achieved

ideal unlearning by masking out the training signal of TOFU dataset (Maini et al. (2024)) in their corpus from the data perspective. While existing methods often overlook the challenges of continuous unlearning requests and the associated catastrophic degradation of model utility in real-world scenarios, Gao et al. (2025) formalizes the concept of continuous machine unlearning and introduces an unlearning framework based on an out-of-distribution detector. Building upon the Gao et al. (2025) paradigm, our method proposes a more refined LoRA update strategy that enables more precise quantification of unlearning extent.

Out-Of-Distribution Detection. The current methods of OOD detection include one-class SVM based methods Erfani et al. (2016), random forest based methods Mihaylov et al. (2018), Gaussian mixture modeling based methods Laxhammar et al. (2009), and deep learning based OOD detection methods Yang et al. (2024). At the same time, OOD detection based on deep learning has become the mainstream in classification tasks. Among them, Zong et al. (2018) is a method suitable for multi-source time series, which estimates OOD scores by generating low-dimensional representations through deep autoencoders. Xu et al. (2021) extracts features by pre-trained language model and then fits one-class SVM for detection. In addition, Zhou et al. (2023) using ensemble learning, Lang et al. (2022) using pseudo-label, Cao et al. (2024) using outlier exposure, Ouyang et al. (2023) using prefix adjustment and other methods have achieved good results in OOD detection. Gao et al. (2025) incorporates the contrastive entropy loss and Masked Language Modeling (MLM) loss (Jian et al. (2022)), enhances the ability to detect out-of-distribution cases. By studying the unlearning process, we introduced the unlearning alignment loss, thereby enhancing the compatibility between the OOD detector and unlearning.

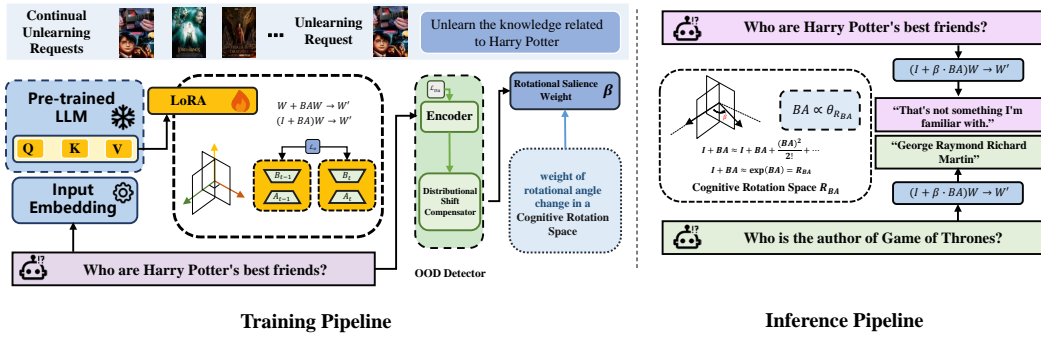


Figure 1: The overall architecture of our method is shown in the figure. In the training pipeline, the orthogonal rotation axes loss \mathcal{L}_o is applied to the attention layers of the LLMs for training; simultaneously, the unlearning alignment loss \mathcal{L}_{Ua} is used to train an OOD detector, whose output is fed into the distributional shift compensator to generate the rotational salience weight β . In the inference pipeline, given that the LoRA parameters BA are proportional to the rotation angle $\theta_{R_{BA}}$ in the Cognitive Rotation Space R_{BA} . We control the rotation angle $\theta_{R_{BA}}$ amplitude by adjusting the scale of LoRA BA , and use the weight β to dynamically load the parameters that match the required unlearning degree.

3 METHODOLOGY

Problem Definition. We use the popular causal LLMs, where the input to the LLM is a sequence of text tokens of variable length. The LLM M_Θ , where Θ is the parameter of the LLM, will calculate the probability of each token in the text under the preorder token based on the input. We set continuous unlearning problem as a series of consecutive arriving unlearning requests, each with $N^{U,t}$ data samples, which can be written as $\{D^{U,t}\}_{t=1}^T$. For the $t - th$ unlearning request, $D^{U,t} = \{x_i || x_i \sim \mathcal{P}_{\mathcal{X}}^{U,t}\}_{i=1}^{N^{U,t}}$, where T is the index of the latest arriving unlearning request, and the P is the input marginal distribution. In each request, we utilize the input $\mathcal{P}_{\mathcal{X}}^t$ and the label distribution $\mathcal{P}_{\mathcal{Y}}^t$ for training. Traditional unlearning methods assume a holdout data set drawn from a distribution $\mathcal{P}_{\mathcal{Y}}^{R,t}$ that is disjoint from the forgetting data set $\mathcal{P}_{\mathcal{X}}^{U,t}$ to preserve the performance of the

162 model on the original training distribution. The immediate goal of continuous unlearning is:
 163

$$164 \sum_{t=1}^T \min_{\Theta^t} \mathbf{I} \left(M_{\mathbf{x} \sim \mathcal{P}_{\mathcal{X}}^{\text{U},t}}(\mathbf{x}, \Theta); M_{\mathbf{x} \sim \mathcal{P}_{\mathcal{X}}^{\text{U},t}}^t(\mathbf{x}, \Theta^t) \right), \sum_{t=1}^T \max_{\Theta^t} \mathbf{I} \left(M_{\mathbf{x} \sim \mathcal{P}_{\mathcal{X}}^{\text{R},t}}(\mathbf{x}, \Theta); M_{\mathbf{x} \sim \mathcal{P}_{\mathcal{X}}^{\text{R},t}}^t(\mathbf{x}, \Theta^t) \right), \quad (1)$$

168 where M^t with the parameters Θ^t represents the target model during and after unlearning on the $t -$
 169 th unlearning set $D_{\text{U},t}^U$, and $I(\cdot; \cdot)$ computes the mutual information between two random variables.
 170 The model utility preservation on other distributions $\mathcal{P}_{\mathcal{X}}^o$ different from the unlearning distribution
 171 is another goal of unlearning. This can be expressed as follows:

$$172 \sum_{t=1}^T \max_{\Theta^t} \mathbf{I} \left(M_{\mathbf{x} \sim \mathcal{P}_{\mathcal{X}}^o}(\mathbf{x}, \Theta); M_{\mathbf{x} \sim \mathcal{P}_{\mathcal{X}}^o}^t(\mathbf{x}, \Theta^t) \right). \quad (2)$$

176 3.1 CONTINUOUS UNLEARNING FOR LLM WITH LORA

178 The continuous unlearning process of LLM inevitably leads to cumulative catastrophic utility loss
 179 (Gao et al. (2025)). The cumulative catastrophic utility loss manifests as a significant decline in
 180 both the LLM’s unlearning capability and its utility retention capability as the number of unlearning
 181 requests increases. At the parameter level, this is reflected in a shift of the parameters corresponding
 182 to previous unlearning requests when the model is trained on new ones. This requires the method to
 183 simultaneously achieve the continuous preservation of its historical unlearning knowledge and the
 184 original utility when handling the current unlearning request.

185 While existing approaches o^3 (Gao et al. (2025)) rely on orthogonal constraints to enforce perpen-
 186 dicularity between parameters of A ($W = BA$). However, this constraint suffers from inherent
 187 limitations: the introduction of parameter B undermines its effectiveness, and its capability further
 188 diminishes as the number of unlearning requests accumulates, making it inadequate for continuous
 189 unlearning scenarios. Moreover, the o^3 empirically assigns weights to LoRA parameters to repre-
 190 sent the degree of unlearning, which is a heuristic design that lacks theoretical grounding and leads
 191 to poor interpretability.

192 We proposed the RCU to address these challenges. We develop a mathematically-derived approach
 193 with enhanced interpretability for quantifying unlearning process. By constructing a cognitive ro-
 194 tation space wherein LLM parameter updates are formulated as a novel rotational transformation,
 195 the RCU transforms continuous unlearning into rotations in a high-dimensional parameter space,
 196 thereby converting uncontrollable parameter shift into controlled angular rotations and ultimately
 197 alleviating cumulative catastrophic utility loss.

198 Our analysis in Figure 2 (a)(b) revealed the relationship between different weighting coefficients
 199 β and unlearning updates, demonstrating that the extent of unlearning intensifies with increasing
 200 values of the β .

201 LoRA Hu et al. (2022) reduces the trainable parameters by introducing two low-rank trainable mat-
 202 rices $\{A, B\}$, where $W_{\text{LoRA}} = BA$, $W_{\text{LoRA}} \in \mathbb{R}^{U \times V}$, $B \in \mathbb{R}^{U \times K}$, $A \in \mathbb{R}^{K \times V}$, which decomposes
 203 the high-dimensional matrix into a low-rank matrix. The specific update formula is as follows:

$$204 W' \leftarrow W + BA. \quad (3)$$

206 LoRA updates inevitably lead to uncontrollable parameter shift. To address this problem, we draw
 207 inspiration from Lie group (Gallier (2001)) to introduce a new update paradigm. This paradigm
 208 redefines parameter updates as rotations within the original parameter space. As rotations are the
 209 rigid transformation (Daniele (2001)), the update via the BA matrices solely governs the change in
 210 the rotation angle. Consequently, the unlearning process is directly driven by changes in this angle,
 211 enabling us to use the rotation angle to precisely quantify the degree of unlearning in LLMs.

212 Firstly, we assume a cognitive rotation space R . Since R can be viewed as an n -dimensional rotation
 213 matrix, R satisfies the following conditions: The R is an orthogonal matrix. The determinant of R
 214 is 1, so $\det(R) = 1$. Since R directly satisfies the two conditions of $SO(n)$, we have $R \in SO(n)$.
 215 From Gallier (2001), we can then conclude that cognitive rotation space $R \in SO(n)$ corresponds to
 216 at least one matrix C in the Lie algebra $\mathfrak{so}(n)$.

216 However, every element C in the Lie algebra $\mathfrak{so}(n)$ can be mapped to the R in the Lie group $SO(n)$
 217 by the exponential map $\exp(C)$. From this we obtain the cognitive rotation space R :

$$218 \quad 219 \quad R = \exp(C), \quad (4)$$

220 here, C is an antisymmetric matrix. Since $R = \exp(C)$, we can obtain from Taylor's Formula:

$$222 \quad 223 \quad R = \exp(C) = I + C + \frac{C^2}{2!} + \dots \approx I + C, C \ll I. \quad (5)$$

224 From Equation 5, we can conclude that for any antisymmetric matrix C , there exists a corresponding
 225 cognitive rotation space R_C . Therefore, we construct the skew symmetric loss \mathcal{L}_{Sk} and impose the
 226 constraint that BA is an antisymmetric matrix:

$$227 \quad 228 \quad \mathcal{L}_{Sk} = \left\| (BA)^T + BA \right\|_F^2, \quad (6)$$

230 here, I is the identity matrix, and $\|\cdot\|_F^2$ is the Frobenius norm.

231 In addition, due to the influence of factors such as the learning rate, $BA \ll I$ (as summarized in
 232 Table 4 and Figure 6 of Appendix A.6, the specifications for the BA matrix parameters are detailed
 233 there.). Thereby, there exists a cognitive rotation space $R_{BA} \approx I + BA$.

234 We can establish the following LoRA update paradigm:

$$235 \quad 236 \quad W \leftarrow W + BAW = (I + BA)W, \quad (7)$$

237 here, we update the above equation given a set of low-rank parameters $\{A, B\}$, where the parameter
 238 matrix W of LLM is frozen.

239 From Equation 7, we can consider the update of the W as a rotation in the cognitive rotation space
 240 R_{BA} .

242 After expressing the update of BA as the cognitive rotation space R_{BA} in the parameter space, we
 243 aim to quantify the degree of unlearning of LLM by changing the rotation angle of R_{BA} .

244 Although we only trained the attention layers, due to the huge parameter size of the large language
 245 model, directly calculating the rotation angle θ of R_{BA} still incurs a significant amount of compu-
 246 tational cost. Here we present our theorem 1.

247 **Theorem 1:** *For $R \in \mathbb{R}^{n \times n}$, when $R = \exp(C)$, the rotation angle θ of R is directly proportional
 248 to C .* The proof of theorem 1 can be found in the appendix.

250 From **Theorem 1**, if we want to change the rotational angle θ of R_{BA} , we only need to make the
 251 corresponding changes to BA . Therefore, we obtain the rotational salience weight β from the OOD
 252 detector and the distributional shift compensator. When $\beta \times BA$, all the rotation angles θ in R_{BA}
 253 are changed to $\beta \times \theta$. Therefore, we can use the rotation Angle θ to quantify the unlearning degree
 254 of LoRA, and only need to use BA for the calculation.

255 In addition, for achieving effective unlearning, we utilize preference optimization to update the
 256 model to accommodate random task labels or refuse-based answers such as "I don't know", which
 257 we call y' . For each unlearning we only train the cross-entropy loss using the unlearning dataset of
 258 our current knowledge:

$$259 \quad 260 \quad \mathcal{L}_{CE} = -\frac{1}{N^{U,t}} \sum_{i=1}^{N^{U,t}} y_i^{U,t} \log M_{\Theta} \left(x_i^{U,t} \right). \quad (8)$$

263 To reduce the interaction between the change of the rotation angle for each unlearning request in
 264 continuous unlearning, we make the rotation axes of each rotation perpendicular to each other. The
 265 rotation axes here refers to the subspace formed by the points that remain stationary under rotation
 266 in the high-dimensional space.

267 Here, we know that when unlearning request t , the corresponding cognitive rotation space is $R_{B_t A_t}$.
 268 Then, from request $t-1$ to request t , the relative rotation matrix is ΔR_t . From this, we can obtain :

$$269 \quad \Delta R_t = R_t \cdot R_{t-1}^T = (I + B_t A_t) (I + B_{t-1} A_{t-1})^T, \quad (9)$$

270 since BA is an antisymmetric matrix, we have:
 271

$$\begin{aligned} 272 \quad \Delta R_t &= (I + B_t A_t) (I + B_{t-1} A_{t-1})^T = (I + B_t A_t) (I - B_{t-1} A_{t-1}) \\ 273 \quad &= I + B_t A_t - B_{t-1} A_{t-1} - B_t A_t B_{t-1} A_{t-1} \approx I + B_t A_t - B_{t-1} A_{t-1}, \\ 274 \end{aligned} \quad (10)$$

275 We cannot directly calculate the rotation axes for the calculation because this would consume a large
 276 amount of computing resources and significantly slow down the training speed of the model. Here,
 277 we know from **Theorem 2** that when the cognitive rotation space $R_{B_{t-1} A_{t-1}}$, $R_{B_t A_t}$ and $B_{t-1} A_{t-1}$,
 278 $B_t A_t$ are mutually perpendicular, their rotation axes must be perpendicular. Therefore, we make the
 279 cognitive rotation space $R_{B_{t-1} A_{t-1}}$ of the $(t-1)$ -th request and the relative rotation space ΔR
 280 relative to the t -th request and the $(t-1)$ -th request mutually perpendicular. This ensures that the
 281 rotation angles of each unlearning request in the cognitive rotation space do not affect each other,
 282 reducing the cumulative catastrophic utility loss generated with continuous unlearning.
 283

284 **Theorem 2:** when $R = \exp(A)$ and $R' = \exp(A')$, $A \perp A'$, then the rotation axes of R and R' are
 285 perpendicular to each other. The proof of theorem 2 can be found in the appendix.

286 We hope that $\Delta R_t = I + B_t A_t - B_{t-1} A_{t-1}$ and $R_{t-1} = I + B_{t-1} A_{t-1}$ are perpendicular to
 287 each other, then $B_t A_t - B_{t-1} A_{t-1}$ and $B_{t-1} A_{t-1}$ will also be perpendicular to each other from
 288 Equation 5 and Theorem 2. The orthogonal rotation axes loss are as follows:

$$289 \quad \mathcal{L}_o = \|(W_t - W_{t-1}) \cdot W_{t-1}\|_F^2 = \|(B_t A_t - B_{t-1} A_{t-1}) \cdot (B_{t-1} A_{t-1})\|_F^2, \quad (11)$$

290 where $W_{t-1} = B_{t-1} A_{t-1}$ are the parameters of the lora after training on the $(t-1)$ -th request. The
 291 $\|\cdot\|_F^2$ is the Frobenius norm.
 292

293 In summary, the overall loss of our method is as follows:
 294

$$295 \quad \mathcal{L}_{overall} = \lambda_1 \mathcal{L}_{Sk} + \lambda_2 \mathcal{L}_o + \lambda_3 \mathcal{L}_{CE}, \quad (12)$$

296 here, we set $\lambda_1 = 0.1, \lambda_2 = 0.1$ and $\lambda_3 = 1$ on the ScienceQA dataset. We set $\lambda_1 = 0.01, \lambda_2 = 0.5$
 297 and $\lambda_3 = 1$ on the TOFU dataset.
 298

300 3.2 UNLEARNED KNOWLEDGE DETECTION

301 **OOD Detection.** Based on o^3 , we turn the unlearned knowledge detection task into an OOD task
 302 by treating the unlearned dataset as In-Distribution (ID) data, and leverage a scoring mechanism to
 303 quantify the extent of unlearning.
 304

305 We propose the OOD detection loss, which consists of three parts. We use the contrastive entropy
 306 loss and Masked Language Modeling (MLM) loss (Gao et al. (2025)). As shown in Figure 2, the
 307 updates of RCU exhibit an uneven characteristic, where the feature always involves continuous
 308 updates within a very small range of rotation angle changes. Given this characteristic, in order to
 309 make the output of OOD detection better align with the update pattern of RCU, we introduced the
 310 unlearning alignment loss \mathcal{L}_{Ua} . The \mathcal{L}_{Ua} are as follows:
 311

$$312 \quad \mathcal{L}_{Ua} = \frac{1}{d^2} \left\| \frac{\hat{Z}_i^T \hat{Z}_i}{n-1} - I \right\|_F^2, \text{ where } \hat{Z}_i = \frac{Z_i}{\|Z_i\|_2}, \quad (13)$$

313 where $\|\cdot\|_2$ is L_2 norm. The Z_i is the average pooled feature representation from layer i of the
 314 backbone network. The $\|\cdot\|_F^2$ denotes the Frobenius norm.
 315

316 In addition, the contrastive entropy \mathcal{L}_{CEL} also starts with the augmentation view generation. The
 317 \mathcal{L}_{CEL} (Gao et al. (2025)) leverage random masking to generate the first view type. For a particular
 318 text instance x with tokens of length n , we randomly select $p\%$ ($p = 15$ in our implementation)
 319 tokens and replace them with the tokens of [MASK]. The x^* is the instance with the random masking.
 320 For the second contrastive view, we make use of a key encoder $F_{\Omega^{key}}$, which is initialized
 321 from the original OOD module backbone F_{Ω} that is a transformer consisting of L attention layers
 322 : $F := f_{\omega_1} \circ \dots \circ f_{\omega_l} \circ \dots \circ f_{\omega_L}$. Then we input the original text instance x and generate the second
 323

324 view from $F_{\Omega^{key}}$. The \mathcal{L}_{CEL} is as follow:

$$\mathcal{L}_{CEL} = - \sum_{i=1}^{N^B} \sum_{l=1}^L \sum_{j=1}^{N^B} \Delta(i, l, j) \log(\Delta(i, l, j)), \quad (14)$$

326
327
328
329
330
331
332
333
334
335
336
337
338
339
340
341
342
343
344
345
346
347
348
349
350
351
352
353
354
355
356
357
358
359
360
361
362
363
364
365
366
367
368
369
370
371
372
373
374
375
376
377

$$\text{where } \Delta(i, l, j) = \frac{\exp \left(f_{\omega_{[1:l]}}(\mathbf{x}_i^*) \cdot f_{\omega_{[1:l]}^{key}}(\mathbf{x}_j) \right)}{\sum_{k=1}^{N^B} \exp \left(f_{\omega_{[1:l]}}(\mathbf{x}_i^*) \cdot f_{\omega_{[1:l]}^{key}}(\mathbf{x}_k) \right)},$$

here N is the sample quantity of a mini-batch. And the $f_{\omega_{[1:l]}}(\mathbf{x}_i^*)$ is the token averaging representation of the l -th layer. We use MLM loss \mathcal{L}_{MLM} (Jian et al. (2022)) to improve the language generation of our model:

$$\mathcal{L}_{MLM} = - \frac{1}{N^B} \sum_{i=1}^{N^B} y_i^* \log F_{\Omega}(\mathbf{x}_i^*), \quad (15)$$

where y^* is the random token masking label. Here, the \mathcal{L}_{CEL} focuses on the relative relationship of sample pairs. The \mathcal{L}_{MLM} boosts the representation power of the generated language.

The final loss \mathcal{L}_{OOD} can be:

$$\mathcal{L}_{OOD} = \mathcal{L}_{CEL} + \mathcal{L}_{MLM} + \mathcal{L}_{Ua}. \quad (16)$$

Distributional Shift Compensator. We follow the method for obtaining the output of OOD detection as described in o^3 . We utilized the Mahalanobis distance and the distance based on the maximum instance cosine similarity. Finally, we calculated the combined score γ^t . For the calculation of the OOD score γ^t , please refer to the appendix.

After we get combined score γ^t , we need to map the γ^t into an rotational salience weight β . Here, we hope that the change of β can conform to the unlearning process of the cognitive rotation space R_{BA} . However, as the unlearning learning proceeds, we find that the performance of the update based on RCU is uneven. As shown in the Figure 2 (a)(b), the model does not learn unlearning knowledge before $\beta = 0.3$ on the ScienceQA dataset. At $\beta = 0.3$ to $\beta = 0.5$, the unlearned knowledge is gradually learned, while at $\beta = 0.5$ to $\beta = 1$, the model has fully learned the unlearned knowledge. On the TOFU dataset, the range of knowledge that the model learns for unlearning is approximately between $\beta = 0.2$ and $\beta = 0.6$. The specific results can be found in the appendix. This gives us the following relation:

$$\beta = \begin{cases} 0.45 & \Gamma_2 < \gamma^t \leq 1, \\ \mathcal{M}(\gamma^t) & \Gamma_1 < \gamma^t \leq \Gamma_2, \\ 0 & \gamma^t \leq \Gamma_1, \end{cases} \quad (17)$$

the Γ_1 and Γ_3 are thresholds, which $\Gamma_1 = 1e-80$, $\Gamma_2 = 0.1$ on the ScienceQA dataset and $\Gamma_1 = 0.2$, $\Gamma_2 = 1$ on the TOFU dataset. The $\mathcal{M}(\gamma^t)$ on the ScienceQA dataset is $0.35 + (\log_{10} \gamma^t + 80) / 790$. The $\mathcal{M}(\gamma^t)$ on the TOFU dataset is $0.35 + ((\gamma^t - 0.2) / 0.8) \cdot 0.25$.

Finally, for each input x of the t -th unlearning request, the corresponding parameters W_x^t can be expressed as:

$$W_x^t = (I + \beta \cdot BA) W. \quad (18)$$

4 EXPERIMENTS

4.1 DATASETS

We conducted experiments on two tasks: question answering and fictional knowledge generation. We have divided the question-answering task into 5 consecutive sub-tasks, and the fictional knowledge generation has been divided into 3 consecutive sub-tasks. The detailed introduction of the datasets is as follows:

Question Answering. We use ScienceQA (Lu et al. (2022)) as the question and answer dataset. This dataset consists of 6,508 training samples and 2,224 testing samples. We selected five of

378 these areas as the continuous unlearning requests, namely biology, physics, chemistry, economics,
 379 and earth-science. We utilized the CommonsenseQA (Talmor et al. (2018)) as the utility dataset,
 380 which contained 9,740 training samples and 1,221 validation samples, to evaluate the commonsense
 381 reasoning ability of LLMs. The OpenbookQA (Taori et al. (2023)) can assess the understanding
 382 ability of books. The training set contains 4,957 samples, the validation set includes 500 samples,
 383 and the test set consists of 500 samples.

384 **Fictitious Knowledge Generation.** We conducted a test on the generation of fictional knowledge
 385 using the TOFU dataset (Maini et al. (2024)). The TOFU dataset contains questions about fictional
 386 authors synthesized by GPT-4. The three unlearning sets 'foget01', 'foget05', and 'foget10' respec-
 387 tively represent random selection ratios of 1%, 5%, and 10% of the authors. The authors in each
 388 unlearning set are mutually exclusive. Additionally, we also utilized the data related to real-word
 389 authors and world facts in this dataset to test the LLMs' ability to maintain its effectiveness.

391 4.2 EXPERIMENTAL SETUP

393 Table 1: Performance Comparison between our method and other baselines when continually un-
 394 learning TOFU-forget01, -forget05, and -forget10 in Fictitious Knowledge Generation. The * rep-
 395 represents the results we achieved in our own experimental environment.

Method	Unlearning Request 1					Unlearning Request 2					Unlearning Request 3				
	S.U.↓	D.U.↓	R.D.↑	R.A.↑	W.F.↑	S.U.↓	D.U.↓	R.D.↑	R.A.↑	W.F.↑	S.U.↓	D.U.↓	R.D.↑	R.A.↑	W.F.↑
Base *	85.0	90.0	85.8	89.0	87.0	87.3	89.3	85.8	89.0	87.0	85.3	90.0	85.8	89.0	87.0
GradASC	75.0	85.0	71.0	86.0	82.1	17.6	23.1	19.0	0	0	17.1	14.2	19.0	0	0
GradDif	78.1	84.0	81.9	86.7	83.5	62.5	70.0	70.4	65.7	77.9	16.5	15.2	19.0	0	0
EUL	84.1	86.3	86.1	86.7	87.1	84.4	90.3	85.8	88.0	85.5	80.1	83.5	83.4	86.3	83.5
PO *	18.75	25.0	77.0	85.0	81.0	31.88	52.5	79.0	86.0	79.0	43.13	52.5	77.75	78.0	80.0
NPO	68.8	75.0	83.6	89.0	81.8	76.3	84.2	83.2	87.7	84.1	77.6	79.2	81.4	87.3	82.9
SOGD	43.7	76.0	80.3	85.3	83.4	22.8	24.0	79.0	81.3	82.6	17.4	21.7	82.3	77.0	82.1
SOP0 *	31.25	37.5	83.7	85.0	83.0	38.13	45.0	80.0	87.0	82.0	36.88	43.75	79.5	85.0	82.0
o^3 *	15.66	14.67	85.25	89.0	86.3	22.49	20.17	85.5	89.0	86.3	26.66	23.56	85.25	89.0	86.3
Ours	9.37	12.5	85.57	89.0	87.0	12.5	85.61	89.0	87.0	20.6	17.5	85.6	89.0	87.0	

406 **Evaluation Metrics.** We continue to use the o^3 (Gao et al. (2025)) key evaluation indicators. Here,
 407 the Sample-level Unlearning (S.U.) represents the performance of the test LLMs on the unlearning
 408 training set when there is a unlearning request. The Distribution-level Unlearning (D.U.) indicates
 409 the performance of the test LLMs on the unlearning test set when there is the unlearning request. In
 410 addition, we use three indicators to measure the performance of the LLMs in maintaining utility. The
 411 Retained Distribution (R.D.) represents the distribution that is most sensitive to unlearning requests.
 412 The CommonsenseQA (C.QA.) and QpenbookQA (O.QA.) are datasets used on the scienceQA
 413 dataset to measure the utility of each request. We use the accuracy of these two datasets to measure
 414 their performance in QA. On the TOFU dataset, we use the utility datasets provided by the two
 415 datasets, namely Real-word Authors (R.A.) and Word Fact (W.F.), to measure their performance in
 416 Fictitious Knowledge Generation.

417 **Compared Baseline.** We compared a series of the most advanced LLM unlearning methods:
 418 GradAsc Golatkhar et al. (2020), GradDif Yao et al. (2024), EUL Chen & Yang (2023a), PO El-
 419 dan & Russinovich (2023), NPO Zhang et al. (2024), SOGD Jia et al. (2024), SOP0 Jia et al. (2024)
 420 and o^3 Gao et al. (2025). The base refers to the result obtained directly through the LLM testing.

421 **Implementation Details.** We use LLaMA2-7b (Touvron et al. (2023)) as the target model. The
 422 detection backbone is Pseudo-Roberta-Large (Liu et al. (2019)). For the TOFU dataset, the learning
 423 rate is 2e-4, and the number of epoch is 10. For the ScienceQA dataset, the batch size is 128, the
 424 number of epoch is 15, and the learning rate is 3e-4. In the inference pipeline of ScienceQA, the max
 425 batch size is 24. The LoRA ranks for both datasets are 8. Our method only fine-tunes the attention
 426 layers in LLM. We conducted our experiments on two NVIDIA RTX A6000.

428 4.3 EXPERIMENTAL RESULTS

430 **Question Answering.** The results of our method are shown in appendix A.8 and Figure 3. We
 431 compared base, PO, SOP0, o^3 and our results. Some detailed results can be found in the appendix.
 Our method achieved the same results as the base method (C.QA. and O.QA.). The results of the

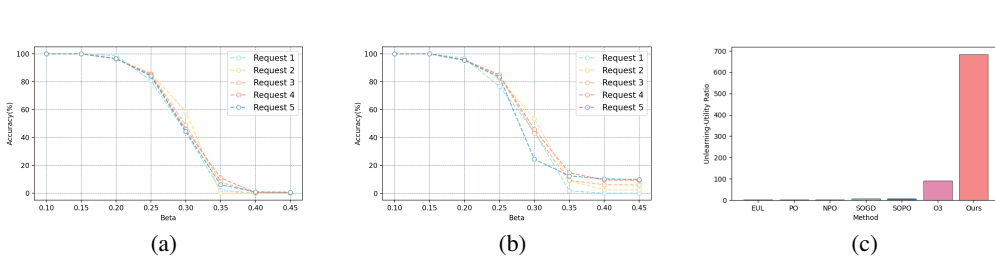


Figure 2: Experimental results on the ScienceQA dataset. (a) The relationship between the β (β is proportional to the rotation angle) and unlearning processes (S.U.). (b) The relationship between the β (β is proportional to the rotation angle) and unlearning processes (D.U.). (c) The results of U^2R on the TOFU dataset.

R.D. were also very similar to those of the base method. However, our method performed much better than the others in the S.U. and D.U. indicators. Compared with the most advanced method o^3 , the S.U. decreased by 9.68%, 4.02%, 4.05%, 7.58% and 10.82% respectively on five requests. The D.U. compared to the most advanced method o^3 , on average, decreased by 17.67% across five requests. In addition, the number of training parameters of our method is much smaller than that of o^3 .

Fictitious Knowledge Generation. Table 1 presents the experimental results of our method on the TOFU dataset. Based on the results, we found that our method can effectively enhance the LLMs' ability to unlearning (D.U. and S.U.). Compared with the currently best continuous unlearning method o^3 , the result on the S.U. decreased by 6.29%, 9.99% and 6.06%. the result on the D.U. decreased by 2.17%, 7.67% and 6.06%. Furthermore, in terms of the stability of the LLMs' utility, the performance level of our method is comparable to the current best results. We observed that as the number of unlearning requests increased, the unlearning accuracy on the test set (D.U.) of most methods showed significant fluctuations or increasing. This phenomenon indicates that catastrophic utility loss continues to accumulate, and the LLMs' stability is affected. In contrast, our method not only effectively mitigates such utility losses but also significantly improves the performance stability of LLMs during the continuous unlearning process.

In two datasets, o^3 has 19.99 M trainable parameters, compared to our method's 8.39 M. The required number of training parameters is significantly less than that of o^3 . The number of parameters that need to be updated in our method is much smaller than that in o^3 .

Furthermore, we follow the Unlearning-Utility Ratio (U^2R) in o^3 .

$$U^2R = \frac{Acc_{S.U.}^0 + Acc_{D.U.}^0 - Acc_{S.U.}^T - Acc_{D.U.}^T}{Acc_{R.D.}^0 + Acc_{U.1}^0 + Acc_{U.2}^0 - Acc_{R.D.}^T - Acc_{U.1}^T - Acc_{U.2}^T}, \quad (19)$$

where the Acc denotes Accuracy, the U.1 represents C.QA or R.A., the U.2 represents O.QA or W.F., and the T denotes the unlearning request. The result on the TOFU dataset is shown in Figure 2 (c). Our method has demonstrated significant advantages in both unlearning and utility retention. Furthermore, the results on the ScienceQA dataset can be found in the Appendix A.2.

4.4 THE RELATIONSHIP BETWEEN ROTATION AND UNLEARNING

In Figure 2 (a) and Figure 2 (b), we have presented the changes about β , along with the experimental results for each unlearning request. Based on the results on the ScienceQA dataset, we can observe that when β is within the range of 0.15 to 0.45, the model rapidly undergoes the process of unlearning. However, when β is less than 0.15, the model does not forget the knowledge. And when β is greater than 0.45, the model has achieved complete forgetting and no longer continues to unlearning. The above experimental results indicate that the unlearning process of RCU is achieved within a very small rotation angle change range in the cognitive rotation space. Therefore, when designing the OOD detector and the distributional shift compensator, we must also ensure that the

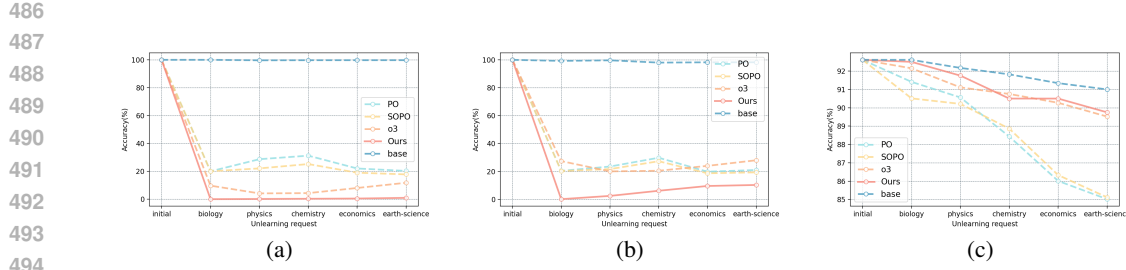


Figure 3: The comparison results with other methods on the ScienceQA dataset. (a) The results of S.U.. (b) The results of D.U.. (c) The results of R.D..

rotational salience weights they output have a relatively concentrated distribution to match the above characteristics. The β changes regarding TOFU dataset are presented in the appendix.

4.5 ABLATION STUDY

The results of our ablation experiments are shown in Table 2. Here, we aim to focus more on the unlearning process rather than the OOD process. Therefore, we consider the impact of \mathcal{L}_{Ua} on the unlearning performance rather than on the OOD performance. Based on the results, we found that \mathcal{L}_{Sk} is the main influencing factor for the unlearning performance. And the LoRA update Paradigm (RC-LoRA in Table 2), \mathcal{L}_{Sk} and the \mathcal{L}_o are three key factors for mitigating cumulative catastrophic utility loss in continuous unlearning. The results of the ablation experiment proved the effectiveness of our method.

Table 2: The ablation experiment results on the ScienceQA dataset. The RC-LoRA represents our LoRA update paradigm.

Method	Unlearning Request 1						Unlearning Request 2						Unlearning Request 3					
	S.U.↓	D.U.↓	R.D.↑	C.QA.↑	O.QA.↑	S.U.↓	D.U.↓	R.D.↑	C.QA.↑	O.QA.↑	S.U.↓	D.U.↓	R.D.↑	C.QA.↑	O.QA.↑	S.U.↓	D.U.↓	R.D.↑
w/o \mathcal{L}_o	0.54	0.68	89.01	79.19	83.09	0.65	4.74	88.02	79.19	83.09	0.78	8.98	88.22	79.19	83.09			
w/o \mathcal{L}_{Sk}	99.75	98.99	90.16	79.19	83.09	99.51	98.01	89.18	79.19	83.09	99.51	98.04	88.44	79.19	83.09			
w/o RC-LoRA	0.12	1.35	90.51	79.19	82.39	0.58	4.24	91.11	79.19	82.39	0.99	22.45	90.68	79.19	82.39			
w/o \mathcal{L}_{Sk} +RC-LoRA	100.00	99.24	89.16	79.19	83.09	99.52	98.14	88.25	79.19	83.09	99.62	98.53	87.44	79.19	83.09			
w/o \mathcal{L}_{Ua}	1.27	3.44	87.01	79.02	81.35	2.77	4.85	88.08	79.02	81.35	3.11	8.23	87.62	79.02	81.35			
Ours	0.05	0.12	92.5	79.19	83.2	0.17	2.45	91.75	79.19	83.2	0.33	6.13	90.5	79.19	83.2			

Method	Unlearning Request 4						Unlearning Request 5						
	S.U.↓	D.U.↓	R.D.↑	C.QA.↑	O.QA.↑	S.U.↓	D.U.↓	R.D.↑	C.QA.↑	O.QA.↑	S.U.↓	D.U.↓	
w/o \mathcal{L}_o	1.24	11.58	88.06	79.19	83.09	2.41	16.85	87.95	79.19	83.09			
w/o \mathcal{L}_{Sk}	99.75	98.04	88.20	79.19	83.09	99.75	98.04	87.95	79.19	83.09			
w/o RC-LoRA	1.03	30.68	89.43	79.19	83.09	2.46	31.85	90.00	79.19	83.09			
w/o \mathcal{L}_{Sk} +RC-LoRA	99.85	98.53	87.2	79.19	83.09	99.85	98.28	86.45	79.19	83.09			
w/o \mathcal{L}_{Ua}	9.19	11.07	87.33	79.02	81.35	13.65	15.21	86.93	79.02	81.35			
Ours	0.49	9.56	90.5	79.19	83.2	0.98	10.29	89.753	79.19	83.2			

5 CONCLUSION

Existing LLM unlearning methods are vulnerable not only to cumulative catastrophic utility loss from continuous unlearning requests, but also to a fundamental limitation in practicality owing to their heavy reliance on the retained dataset. To overcome this limitation, we introduce RCU, a retain-free approach that formulates LoRA updates as rotations within a specially constructed cognitive rotation space. This formulation makes the rotational angle updated by LoRA the sole variable, which is strongly correlated with the degree of unlearning. Consequently, the unlearning process can be directly quantified by corresponding changes in the rotational angle. Furthermore, by analyzing the update dynamics during unlearning, we propose a rotational salience weight to achieve precise and continuous control over the unlearning process. Our method is supported by theoretical guarantees, and we rigorously establish its efficacy through a mathematical analysis. Extensive experiments demonstrate that RCU achieves superior unlearning effectiveness while maintaining model utility on multiple datasets.

540 REFERENCES
541

542 Josh Achiam, Steven Adler, Sandhini Agarwal, Lama Ahmad, Ilge Akkaya, Florencia Leoni Ale-
543 man, Diogo Almeida, Janko Altenschmidt, Sam Altman, Shyamal Anadkat, et al. Gpt-4 technical
544 report. *arXiv preprint arXiv:2303.08774*, 2023.

545 Lucas Bourtoule, Varun Chandrasekaran, Christopher A Choquette-Choo, Hengrui Jia, Adelin
546 Travers, Baiwu Zhang, David Lie, and Nicolas Papernot. Machine unlearning. In *2021 IEEE*
547 *symposium on security and privacy (SP)*, pp. 141–159. IEEE, 2021.

548 Jan Bronec and Jindřich Helcl. Atyaephyra at semeval-2025 task 4: Low-rank negative preference
549 optimization. *arXiv preprint arXiv:2503.13690*, 2025.

550 Chentao Cao, Zhun Zhong, Zhanke Zhou, Yang Liu, Tongliang Liu, and Bo Han. Envision-
551 ing outlier exposure by large language models for out-of-distribution detection. *arXiv preprint*
552 *arXiv:2406.00806*, 2024.

553 Jiaao Chen and Diyi Yang. Unlearn what you want to forget: Efficient unlearning for llms. *arXiv*
554 *preprint arXiv:2310.20150*, 2023a.

555 Jiaao Chen and Diyi Yang. Unlearn what you want to forget: Efficient unlearning for llms. *arXiv*
556 *preprint arXiv:2310.20150*, 2023b.

557 Yiwei Chen, Yuguang Yao, Yihua Zhang, Bingquan Shen, Gaowen Liu, and Sijia Liu. Safety mirage:
558 How spurious correlations undermine vlm safety fine-tuning. *arXiv preprint arXiv:2503.11832*,
559 2025.

560 Ronen Eldan and Mark Russinovich. Who's harry potter? approximate unlearning for llms. 2023.

561 Sarah M Erfani, Sutharshan Rajasegarar, Shanika Karunasekera, and Christopher Leckie. High-
562 dimensional and large-scale anomaly detection using a linear one-class svm with deep learning.
563 *Pattern Recognition*, 58:121–134, 2016.

564 Jean Gallier. Basics of classical lie groups: The exponential map, lie groups, and lie algebras.
565 In *Geometric Methods and Applications: For Computer Science and Engineering*, pp. 367–414.
566 Springer, 2001.

567 Chongyang Gao, Lixu Wang, Kaize Ding, Chenkai Weng, Xiao Wang, and Qi Zhu. On large lan-
568 guage model continual unlearning. In *The Thirteenth International Conference on Learning Rep-*
569 *resentations*, 2025.

570 Aditya Golatkar, Alessandro Achille, and Stefano Soatto. Eternal sunshine of the spotless net:
571 Selective forgetting in deep networks. In *Proceedings of the IEEE/CVF conference on computer*
572 *vision and pattern recognition*, pp. 9304–9312, 2020.

573 Estrid He, Tabinda Sarwar, Ibrahim Khalil, Xun Yi, and Ke Wang. Deep contrastive unlearning for
574 language models. *arXiv preprint arXiv:2503.14900*, 2025.

575 Linxi Zhao, Sofian Zalouk, Christian K. Belardi, Justin Lovelace, Jin Peng Zhou, Kilian Q. Wein-
576 berger, Yoav Artzi, Jennifer J. Sun. Pre-training Large Memory Language Models with Internal
577 and External Knowledge. *arXiv preprint arXiv:2505.15962*, 2025.

578 Daniele Mortari. On the rigid rotation concept in n-dimensional spaces. In *The Journal of the*
579 *astronautical sciences*, pp. 401–420. Springer, 2001.

580 Edward J Hu, Yelong Shen, Phillip Wallis, Zeyuan Allen-Zhu, Yuanzhi Li, Shean Wang, Lu Wang,
581 Weizhu Chen, et al. Lora: Low-rank adaptation of large language models. *ICLR*, 1(2):3, 2022.

582 Jinwei Hu, Zhenglin Huang, Xiangyu Yin, Wenjie Ruan, Guangliang Cheng, Yi Dong, and Xiaowei
583 Huang. Falcon: Fine-grained activation manipulation by contrastive orthogonal unalignment for
584 large language model. *arXiv preprint arXiv:2502.01472*, 2025.

585 Jinghan Jia, Yihua Zhang, Yimeng Zhang, Jiancheng Liu, Bharat Runwal, James Diffenderfer,
586 Bhavya Kailkhura, and Sijia Liu. Soul: Unlocking the power of second-order optimization for
587 llm unlearning. *arXiv preprint arXiv:2404.18239*, 2024.

594 Yiren Jian, Chongyang Gao, and Soroush Vosoughi. Contrastive learning for prompt-based few-shot
 595 language learners. *arXiv preprint arXiv:2205.01308*, 2022.

596

597 Peihai Jiang, Xixiang Lyu, Yige Li, and Jing Ma. Backdoor token unlearning: Exposing and de-
 598 fending backdoors in pretrained language models. In *Proceedings of the AAAI Conference on*
 599 *Artificial Intelligence*, volume 39, pp. 24285–24293, 2025.

600 Hao Lang, Yinhe Zheng, Jian Sun, Fei Huang, Luo Si, and Yongbin Li. Estimating soft labels for
 601 out-of-domain intent detection. *arXiv preprint arXiv:2211.05561*, 2022.

602

603 Rikard Laxhammar, Goran Falkman, and Egils Sviestins. Anomaly detection in sea traffic-a com-
 604 parison of the gaussian mixture model and the kernel density estimator. In *2009 12th international*
 605 *conference on information fusion*, pp. 756–763. IEEE, 2009.

606

607 Aixin Liu, Bei Feng, Bing Xue, Bingxuan Wang, Bochao Wu, Chengda Lu, Chenggang Zhao,
 608 Chengqi Deng, Chenyu Zhang, Chong Ruan, et al. Deepseek-v3 technical report. *arXiv preprint*
 609 *arXiv:2412.19437*, 2024.

610

611 Sijia Liu, Yuanshun Yao, Jinghan Jia, Stephen Casper, Nathalie Baracaldo, Peter Hase, Yuguang
 612 Yao, Chris Yuhao Liu, Xiaojun Xu, Hang Li, et al. Rethinking machine unlearning for large
 613 language models. *Nature Machine Intelligence*, pp. 1–14, 2025.

614

615 Yinhan Liu, Myle Ott, Naman Goyal, Jingfei Du, Mandar Joshi, Danqi Chen, Omer Levy, Mike
 616 Lewis, Luke Zettlemoyer, and Veselin Stoyanov. Roberta: A robustly optimized bert pretraining
 617 approach. *arXiv preprint arXiv:1907.11692*, 2019.

618

619 Pan Lu, Swaroop Mishra, Tanglin Xia, Liang Qiu, Kai-Wei Chang, Song-Chun Zhu, Oyvind Tafjord,
 620 Peter Clark, and Ashwin Kalyan. Learn to explain: Multimodal reasoning via thought chains for
 621 science question answering. *Advances in Neural Information Processing Systems*, 35:2507–2521,
 622 2022.

623

624 Pratyush Maini, Zhili Feng, Avi Schwarzschild, Zachary C Lipton, and J Zico Kolter. Tofu: A task
 625 of fictitious unlearning for llms. *arXiv preprint arXiv:2401.06121*, 2024.

626

627 Todor Mihaylov, Peter Clark, Tushar Khot, and Ashish Sabharwal. Can a suit of armor conduct
 628 electricity? a new dataset for open book question answering. *arXiv preprint arXiv:1809.02789*,
 629 2018.

630

631 Aashiq Muhammed, Jacopo Bonato, Mona T Diab, and Virginia Smith. Saes can improve unlearning:
 632 Dynamic sparse autoencoder guardrails for precision unlearning in llms. In *ICML 2025 Workshop*
 633 *on Reliable and Responsible Foundation Models*, 2025.

634

635 Guillermo Ortiz-Jimenez, Alessandro Favero, and Pascal Frossard. Task arithmetic in the tangent
 636 space: Improved editing of pre-trained models. *Advances in Neural Information Processing Sys-*
 637 *tems*, 36:66727–66754, 2023.

638

639 Yawen Ouyang, Yongchang Cao, Yuan Gao, Zhen Wu, Jianbing Zhang, and Xinyu Dai. On prefix-
 640 tuning for lightweight out-of-distribution detection. In *Proceedings of the 61st Annual Meeting of*
 641 *the Association for Computational Linguistics (Volume 1: Long Papers)*, pp. 1533–1545, 2023.

642

643 Xudong Pan, Mi Zhang, Shouling Ji, and Min Yang. Privacy risks of general-purpose language
 644 models. In *2020 IEEE Symposium on Security and Privacy (SP)*, pp. 1314–1331. IEEE, 2020.

645

646 Iraklis Prempjis, Maria Lymperaiou, Giorgos Filandrianos, Orfeas Menis Mastromichalakis,
 647 Athanasios Voulodimos, and Giorgos Stamou. Ails-ntua at semeval-2025 task 4: Parameter-
 648 efficient unlearning for large language models using data chunking. *arXiv preprint*
 649 *arXiv:2503.02443*, 2025.

650

651 Alon Talmor, Jonathan Herzig, Nicholas Lourie, and Jonathan Berant. Commonsenseqa: A question
 652 answering challenge targeting commonsense knowledge. *arXiv preprint arXiv:1811.00937*, 2018.

653

654 Rohan Taori, Ishaan Gulrajani, Tianyi Zhang, Yann Dubois, Xuechen Li, Carlos Guestrin,
 655 Percy Liang, and Tatsunori B Hashimoto. Alpaca: A strong, replicable instruction-
 656 following model. *Stanford Center for Research on Foundation Models*. <https://crfm.stanford.edu/2023/03/13/alpaca.html>, 3(6):7, 2023.

648 Pratiksha Thaker, Yash Maurya, Shengyuan Hu, Zhiwei Steven Wu, and Virginia Smith. Guardrail
 649 baselines for unlearning in llms. *arXiv preprint arXiv:2403.03329*, 2024.
 650

651 Hugo Touvron, Louis Martin, Kevin Stone, Peter Albert, Amjad Almahairi, Yasmine Babaei, Niko-
 652 lay Bashlykov, Soumya Batra, Prajjwal Bhargava, Shruti Bhosale, et al. Llama 2: Open founda-
 653 tion and fine-tuned chat models. *arXiv preprint arXiv:2307.09288*, 2023.
 654

655 Lei Wang, Chen Ma, Xueyang Feng, Zeyu Zhang, Hao Yang, Jingsen Zhang, Zhiyuan Chen, Jiakai
 656 Tang, Xu Chen, Yankai Lin, et al. A survey on large language model based autonomous agents.
 657 *Frontiers of Computer Science*, 18(6):186345, 2024.
 658

659 Qizhou Wang, Jin Peng Zhou, Zhanke Zhou, Saebyeol Shin, Bo Han, and Kilian Q Weinberger.
 660 Rethinking llm unlearning objectives: A gradient perspective and go beyond. *arXiv preprint
 661 arXiv:2502.19301*, 2025a.
 662

663 Wenyu Wang, Mengqi Zhang, Xiaotian Ye, Zhaochun Ren, Zhumin Chen, and Pengjie Ren. Uipe:
 664 Enhancing llm unlearning by removing knowledge related to forgetting targets. *arXiv preprint
 665 arXiv:2503.04693*, 2025b.
 666

667 Keyang Xu, Tongzheng Ren, Shikun Zhang, Yihao Feng, and Caiming Xiong. Unsupervised out-
 668 of-domain detection via pre-trained transformers. *arXiv preprint arXiv:2106.00948*, 2021.
 669

670 Jingkang Yang, Kaiyang Zhou, Yixuan Li, and Ziwei Liu. Generalized out-of-distribution detection:
 671 A survey. *International Journal of Computer Vision*, 132(12):5635–5662, 2024.
 672

673 Puning Yang, Qizhou Wang, Zhuo Huang, Tongliang Liu, Chengqi Zhang, and Bo Han. Exploring
 674 criteria of loss reweighting to enhance llm unlearning. *arXiv preprint arXiv:2505.11953*, 2025.
 675

676 Yuanshun Yao, Xiaojun Xu, and Yang Liu. Large language model unlearning. *Advances in Neural
 677 Information Processing Systems*, 37:105425–105475, 2024.
 678

679 Biao Yi, Tiansheng Huang, Baolei Zhang, Tong Li, Lihai Nie, Zheli Liu, and Li Shen. Ctrap:
 680 Embedding collapse trap to safeguard large language models from harmful fine-tuning. *arXiv
 681 preprint arXiv:2505.16559*, 2025.
 682

683 Miao Yu, Liang Lin, Guibin Zhang, Xinfeng Li, Junfeng Fang, Ningyu Zhang, Kun Wang, and Yang
 684 Wang. Unierase: Unlearning token as a universal erasure primitive for language models. *arXiv
 685 preprint arXiv:2505.15674*, 2025.
 686

687 Ruiqi Zhang, Licong Lin, Yu Bai, and Song Mei. Negative preference optimization: From catas-
 688 trophic collapse to effective unlearning. *arXiv preprint arXiv:2404.05868*, 2024.
 689

690 Yunhua Zhou, Jianqiang Yang, Pengyu Wang, and Xipeng Qiu. Two birds one stone: Dynamic en-
 691 semble for ood intent classification. In *Proceedings of the 61st Annual Meeting of the Association
 692 for Computational Linguistics (Volume 1: Long Papers)*, pp. 10659–10673, 2023.
 693

694 Bo Zong, Qi Song, Martin Renqiang Min, Wei Cheng, Cristian Lumezanu, Daeki Cho, and Haifeng
 695 Chen. Deep autoencoding gaussian mixture model for unsupervised anomaly detection. In *Inter-
 696 national conference on learning representations*, 2018.
 697

698

699 **A APPENDIX**
 700

701 This Appendix includes additional details for the our paper including the following aspects:
 702

- A.1: The proofs of the theorem 1 and theorem 2.
- A.2: Detailed experimental results on the ScienceQA dataset.
- A.3: Large Language Model usage declaration.
- A.4: The experimental results on the TOFU dataset showing the relationship between β and the unlearning process.
- A.5: The detailed calculation steps of the OOD Score.

- A.6: An in-depth study on why our method is effective.
- A.7: Experimental results regarding the hyperparameter λ
- A.8: Computation overhead analysis.
- A.9: The comparison results of the Truth Ratio on the TOFU dataset.

A.1 PROOFS OF THE THEOREMS.

Theorem 1: For $R \in \mathbb{R}^{n \times n}$, when $R = \exp(C)$, the rotation angle θ of R is directly proportional to C .

Proof 1: It is known that $R \in SO(n)$ is an n -dimensional rotation matrix ($n > 3$) and $R = \exp(C)$, where C is an antisymmetric matrix. If the rotation angle of $R = \exp(C)$ is θ , then the rotation Angle of $\exp(kC)$ is $k\theta$.

Due to $R \in SO(n)$, there exist orthogonal matrices Q such that:

$$R = Q \cdot \text{diag}(1, \dots, 1.R(\theta_1), \dots, R(\theta_m)) \cdot Q^T, \quad (20)$$

here, $R = \begin{bmatrix} \cos \theta_j & -\sin \theta_j \\ \sin \theta_j & \cos \theta_j \end{bmatrix}$ is Two-dimensional rotation matrix (the rotation angle is θ_j), the rest of the eigenvalues are 1. The $m = [n/2]$.

The antisymmetric matrix C can be similarly block-diagonalized as follows:

$$C = Q \cdot \text{diag}(0, \dots, 0, B(\theta_1), \dots, B(\theta_m)) \cdot Q^T, \quad (21)$$

where $B = \begin{bmatrix} 0 & -\theta_j \\ \theta_j & 0 \end{bmatrix} \cdot \exp(B(\theta_j)) = R(\theta_j)$.

If $C' = kC$, we can gather:

$$C' = Q \cdot \text{diag}(0, \dots, 0, B(\theta_1), \dots, B(\theta_m)) \cdot Q^T, \quad (22)$$

since B is linear, $B(k\theta_j) = kB(\theta_j)$. Then:

$$\begin{aligned} \exp(kC) &= \exp(C') = Q \cdot \exp(\text{diag}(0, \dots, 0, B(k\theta_1), \dots, B(k\theta_m))) \cdot Q^T \\ &= Q \cdot \text{diag}(1, \dots, 1.B(k\theta_1), \dots, B(k\theta_m)) \cdot Q^T. \end{aligned} \quad (23)$$

And the $\exp(B(k\theta_j))$ is as follow:

$$\exp(B(k\theta_j)) = \begin{bmatrix} \cos(k\theta_j) & -\sin(k\theta_j) \\ \sin(k\theta_j) & \cos(k\theta_j) \end{bmatrix} = R(k\theta_j). \quad (24)$$

Due to the Equation 25 and Equation 24, we can get as follow:

$$\exp(kC) = Q \cdot \text{diag}(0, \dots, 0, R(k\theta_1), \dots, R(k\theta_m)) \cdot Q^T, \quad (25)$$

here means the rotation angle of $\exp(kC)$ are $k\theta_1, \dots, k\theta_m$.

Theorem 2: when $R = \exp(A)$ and $R' = \exp(A')$, $A \perp A'$, then the rotation axes of R and R' are perpendicular to each other.

Proof 2: Let A and A' be skew-symmetric matrices with their rotation faces P and P' , respectively. Assume that P and P' are orthogonal to each other (A and A' are perpendicular). Since $P \perp P'$, there are $P \subseteq \ker(A')$ and $P' \subseteq \ker(A)$. (Here, $\ker(\cdot)$ refers to the null space.) Thus, for any vector v , $A'Av = 0$ and $AA'v = 0$, which is $AA' = A'A = 0$.

Now, $R = \exp(A) = I + A + \frac{A^2}{2!} + \dots$. Similarly, $R' = \exp(A')$.

The rotation face of R is P (the eigenspace corresponding to the nonzero eigenvalues of A), since $\exp(A)$ is the usual rotation on P and identity elsewhere. Similarly, the surface of rotation of R' is P' . Since P and P' are orthogonal, the spaces of rotation of R and R' are perpendicular to each other.

Thus, when the rotation faces of the skewsymmetric matrices A and A' generating rotations are perpendicular to each other, the rotation spaces of the corresponding rotation matrices R' and R are also perpendicular to each other.

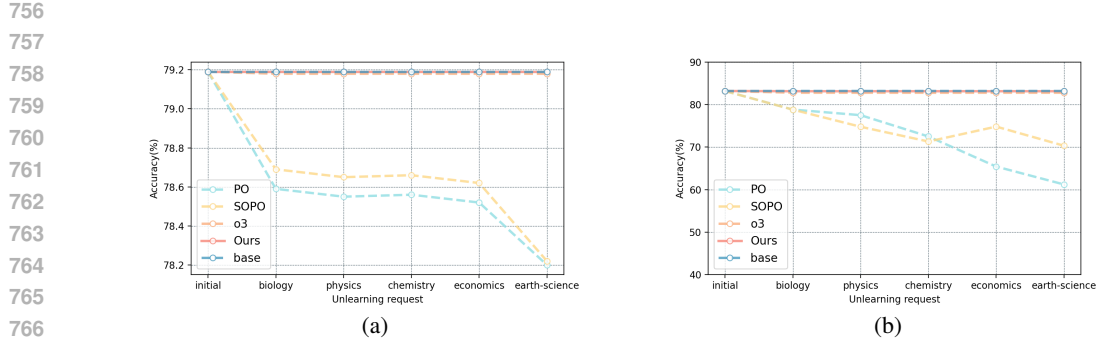


Figure 4: Experimental results on the ScienceQA dataset. (a) The results of C.QA.. (b)The results of O.QA..

A.2 MORE EXPERIMENTAL RESULTS

The detailed results of our work on the ScienceQA dataset are shown in Table 3. Based on the results, we can observe that compared to σ^3 , our method is more stable and has a better ability to resist cumulative catastrophic utility loss. Here, the U^2R of our method is 65.79, and the U^2R of the other method is 48.46.

Table 3: Performance Comparison between our method and other baselines when continually unlearning biology, physics, chemistry, economics and earth-science in Fictitious Knowledge Generation. The unlearning effectiveness is measured by the generation accuracy of the unlearning train data and unlearning test data denoted as S.U. and D.U., CommonsenseQA (C.QA.), OpenbookQA (O.QA.) respectively. Utility preservation is evaluated by the generation accuracy of Retained Distribution (R.D.). The * represents the results we achieved in our own experimental environment.

Method	Unlearning Request 1					Unlearning Request 2					Unlearning Request 3				
	S.U.↓	D.U.↓	R.D.↑	C.QA.↑	O.QA.↑	S.U.↓	D.U.↓	R.D.↑	C.QA.↑	O.QA.↑	S.U.↓	D.U.↓	R.D.↑	C.QA.↑	O.QA.↑
Base *	100	99.24	92.61	79.19	83.2	99.66	98.3	92.17	79.192	83.2	99.73	98.02	91.82	79.19	83.2
σ^3 *	9.73	27.4	92.15	79.19	83.0	4.19	20.03	91.11	79.19	83.0	4.38	20.48	90.25	79.19	83.0
Ours	0.05	0.12	92.5	79.19	83.2	0.17	2.45	91.75	79.19	83.2	0.33	6.13	90.5	79.19	83.2

Method	Unlearning Request 4					Unlearning Request 5				
	S.U.↓	D.U.↓	R.D.↑	C.QA.↑	O.QA.↑	S.U.↓	D.U.↓	R.D.↑	C.QA.↑	O.QA.↑
Base	99.75	98.23	91.34	79.19	83.2	99.77	98.25	91.0	79.19	83.2
σ^3	8.07	23.98	90.17	79.19	83.0	11.8	28.0	89.52	79.19	83.0
Ours	0.49	9.56	90.5	79.19	83.2	0.98	10.29	89.753	79.19	83.2

The specific results are shown in Figure 4.

A.3 LARGE LANGUAGE MODEL USAGE DECLARATION

During this research process, the LLM provided significant assistance in organizing the logic of the paper and improving the language expression. Here, we express our gratitude for the role that the LLM played in enhancing the logicality and clarity of this research.

A.4 HYPERPARAMETER ANALYSIS ON THE TOFU DATASET

The results on TOFU dataset are shown in Figure 5. We found that the change of β shifted slightly to the right for a short period, but the overall change was still concentrated in a certain area. Therefore, when designing the distributional shift compensator for TOFU dataset, we also tried to map $\mathcal{M}(\gamma^t)$ to the range of 0.2 to 0.6.

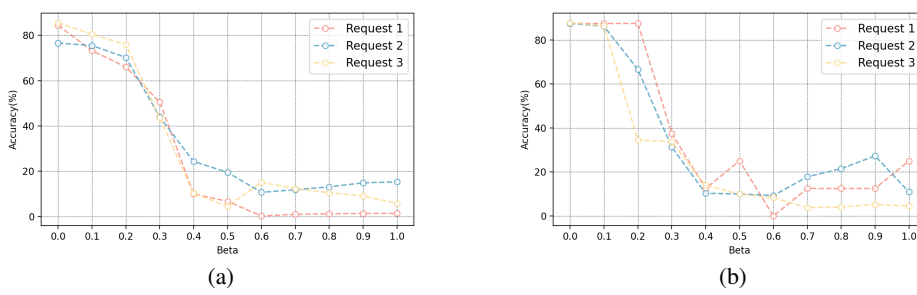


Figure 5: The relationship between the β process and the unlearning process. (a) The results of S.U. on the TOFU dataset. (b) The results of D.U. on the TOFU dataset.

A.5 CALCULATION OF OOD SCORE

We follow the method for obtaining the output of OOD detection as described in o^3 . Our method for calculating the OOD score is as follows:

$$s(x)_l = (f_{w[1:l]} - \mu_l)^T \sum_l^{-1} (f_{w[1:l]} - \mu_l) + \gamma \cdot \left(-\max_{i=1}^{\alpha N^U} \left\{ \frac{f_{w[1:l]}(x) \cdot f_{w[1:l]}(x_i^U)}{|f_{w[1:l]}(x)| |f_{w[1:l]}(x_i^U)|} \right\} \right), \quad (26)$$

$$\mu_l = \frac{1}{\alpha N^U} \sum_{i=1}^{\alpha N^U} f_{w[1:l]}(x_i^U), \Sigma_l = \frac{1}{\alpha N^U} \sum_{i=1}^{\alpha N^U} (f_{w[1:l]}(x_i^U) - \mu_l) (f_{w[1:l]}(x_i^U) - \mu_l)^T, \quad (27)$$

here, $r = 1000$, f_{w_l} representing the parameter of layer l . $D_{used}^{U,t}$ refers to one of the two subsets randomly divided from the training dataset $D^{U,t}$, which contains $\alpha N^{U,t}$ samples.

When the T -th re-learning request is completed, each test input x is input into the OOD detection to calculate the score vector, and the distance between x and the hyper-spherical $\mathcal{H}^t(c^t, r^t)$ boundary is obtained using one-class SVM. The final score is:

$$d_{\mathcal{H}^t}(x) = |s(x)^t - c^t| - r^t, \quad (28)$$

$$\gamma^t = \delta \{ \zeta [1 - \max(p, p') + \min(p, p')] \}, p = \mathcal{P}_{\text{mix}}^t(d_{\mathcal{H}^t}(x)), p' = \mathcal{P}_{\text{mix}}^t(2 d_{\mathcal{H}^t}^0 - d_{\mathcal{H}^t}(x)), \quad (29)$$

here, c^t and r^t represent the center vector and radius of the hypersphere. \mathcal{P}_{mix} is the mixed gaussian distribution function.

A.6 RESEARCH ON OUR METHOD

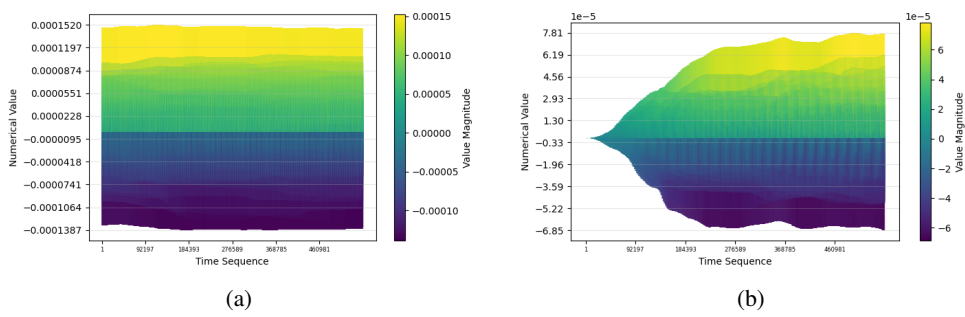
Starting from the intrinsic characteristics of the model parameters, we analyzed the proposed method. Specifically, the magnitude of the learnable parameter Θ_{BA} in each training round is shown in Table 4. The study found that when the parameters $\Theta_{BA} \ll 1$, the matrix $I + BA$ always has a corresponding cognitive rotation space. In the ablation experiments (Table 2), when we remove the designed LoRA update paradigm, the unlearning effect measured by D.U. is relatively ideal when

Table 4: On the ScienceQA dataset, the parameter Θ_{BA} maintained a stable performance at the 10^{-6} scale in multiple unlearning requests (block 1 in attention layers)

Unlearning Request	Param B	Param A
biology	10^{-6}	10^{-5}
physics	10^{-5}	10^{-5}
chemistry	10^{-5}	10^{-5}
economics	10^{-6}	10^{-5}
earth-science	10^{-6}	10^{-5}

864 the unlearning request is 1 to 2. How-
 865 ever, when the unlearning request reached 3 or higher, due to the cumulative catastrophic utility
 866 loss, the unlearning performance reflected by D.U. significantly decreased. The core of this method
 867 lies in introducing the Lsk loss, which can constrain the parameters Θ_{BA} to continuously maintain a
 868 small amplitude, thereby maintaining the effectiveness of the cognitive rotation space and ensuring
 869 the continuous efficacy of the method in handling the continuous unlearning. The results shown in
 870 Table 4 pertain to the queries layer of the attention layers (block 1). The other results generally vary
 871 within the range of 10^{-6} to 10^{-5} .

872 Furthermore, Figure 6 (a)(b) present the evolution of parameters Θ_A and Θ_B throughout the experi-
 873 ment. The results indicate that the magnitudes of both Θ_A and Θ_B remain significantly smaller than
 874 those of parameter I during the entire training process.



877 Figure 6: The results of 5 continuous unlearning processes on the ScienceQA dataset. (a) The
 878 changes in the Θ_A . (b) The changes in the Θ_B .

890 A.7 HYPERPARAMETER ANALYSIS

892 We conducted a comprehensive hyperparameter analysis on λ_1 , λ_2 , and λ_3 across two datasets. The
 893 results, presented in Figure 7 and Figure 8, demonstrate that our chosen hyperparameter configura-
 894 tion consistently achieves optimal performance.

896 A.8 COMPUTATION OVERHEAD ANALYSIS.

898 During the reasoning process, the computational cost for LLM to update using the lora update
 899 paradigm proposed by us is 45.10 GFLOPs, the computational cost for OOD Detection is 709
 900 MFLOPs, and the computational cost for the Distributional Shift Compensator is 13255 MFLOPs.
 901 The total computational cost is 59.064 GFLOPs. In addition, our method requires less storage space.
 902 The storage space required by lora in o^3 is 39MB, while our method only requires 16MB, reducing
 903 the additional storage space requirement by 58%.

904 A.9 THE COMPARISON RESULTS OF THE EVALUATION INDICATORS ON THE TOFU DATASET.

906 We choose the Truth Ratio and ROUGE-L as the indicators for evaluating the utility on the TOFU
 907 dataset.

909 The results of the Truth Ratio (Maini et al. (2024)) are presented in Table 5. From these results, it
 910 can be seen that our method is superior to the comparison methods. The formula for the Truth Ratio
 911 is as shown in Equation 30.

$$912 R_{\text{truth}} = \frac{\frac{1}{|\mathcal{A}_{\text{pert}}|} \sum_{\tilde{a} \in \mathcal{A}_{\text{pert}}} P(\tilde{a} | q)^{1/|\tilde{a}|}}{P(\tilde{a} | q)^{1/|\tilde{a}|}}, \quad (30)$$

914 where \tilde{a} is a paraphrased version of the correct original answer a , $\tilde{a} \in \mathcal{A}_{\text{pert}}$ are deliberately per-
 915 turbed (incorrect) answers derived from \tilde{a} , and $|\tilde{a}|$ denotes the number of tokens in \tilde{a} .

917 We compute the ROUGE-L recall score (Maini et al. (2024)), which acts as a surrogate for accuracy
 918 on the question answering task, as it accounts for the output phrasing to be slightly different than

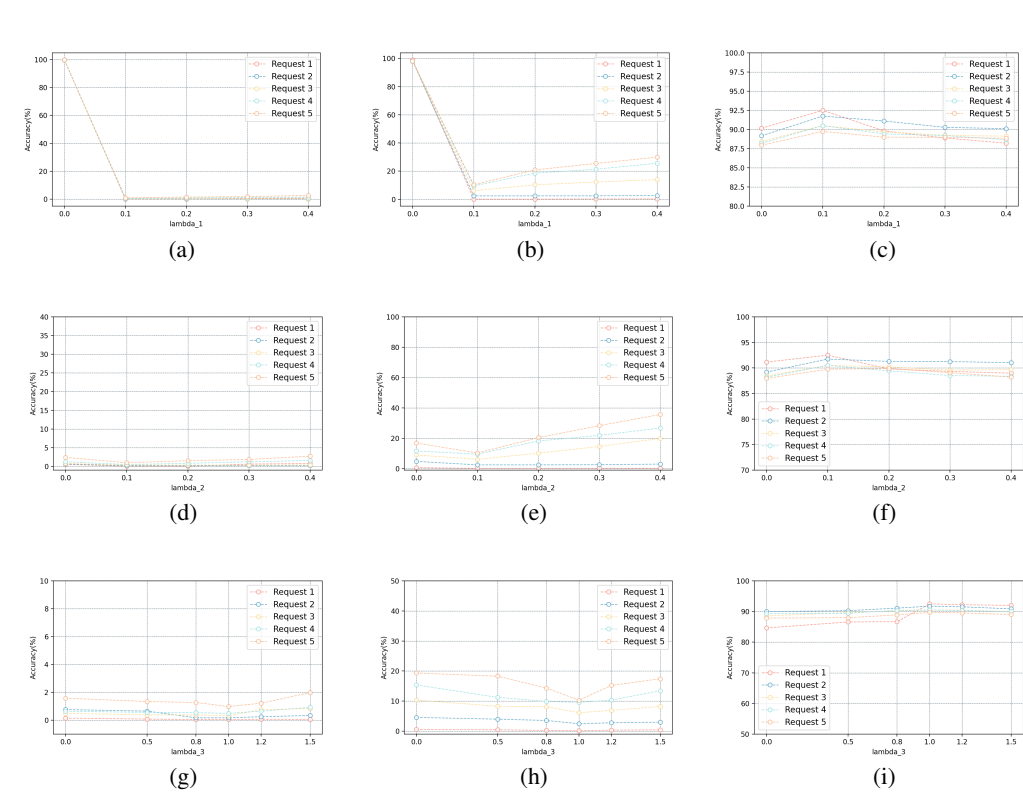


Figure 7: Experimental results on the ScienceQA dataset. The left column shows the results of S.U., the middle column shows the results of D.U., and the right column shows the results of R.D.. (a) (b) (c) The result of the hyperparameter λ_1 . (d) (e) (f) The result of the hyperparameter λ_2 (S.U.). (g) (h) (i) The result of the hyperparameter λ_3 (S.U.).

Table 5: The results here are all the Truth Ratio (Maini et al. (2024)) corresponding to the aforementioned indicators.

Method Truth Ratio	Unlearning Request 1					Unlearning Request 2					Unlearning Request 3				
	S.U. \uparrow	D.U. \uparrow	R.D. \downarrow	R.A. \downarrow	W.F. \downarrow	S.U. \uparrow	D.U. \uparrow	R.D. \downarrow	R.A. \downarrow	W.F. \downarrow	S.U. \uparrow	D.U. \uparrow	R.D. \downarrow	R.A. \downarrow	W.F. \downarrow
o^3	0.74	0.66	0.57	0.54	1.54	0.65	0.65	0.57	0.54	1.54	0.66	0.65	0.57	0.54	1.54
Ours	1.00	1.11	0.56	0.54	1.22	0.99	0.97	0.56	0.54	1.22	0.97	1.01	0.56	0.54	1.22

the ground truth. The results of the ROUGE-L (Maini et al. (2024)) are presented in Table 6. From these results, it can be seen that our method is superior to the comparison methods.

Table 6: The results here are all the ROUGE-L (Maini et al. (2024)) corresponding to the aforementioned indicators.

Method ROUGE-L	Unlearning Request 1					Unlearning Request 2					Unlearning Request 3				
	S.U. \downarrow	D.U. \downarrow	R.D. \uparrow	R.A. \uparrow	W.F. \uparrow	S.U. \downarrow	D.U. \downarrow	R.D. \uparrow	R.A. \uparrow	W.F. \uparrow	S.U. \downarrow	D.U. \downarrow	R.D. \uparrow	R.A. \uparrow	W.F. \uparrow
o^3	0.0771	0.0627	0.9675	0.9330	0.8960	0.1939	0.1255	0.9677	0.9330	0.8960	0.1843	0.5189	0.9675	0.9330	0.8960
Ours	0.0425	0.0365	0.9675	0.9330	0.9083	0.1333	0.1044	0.9683	0.9330	0.9083	0.1322	0.1062	0.9683	0.9330	0.9083

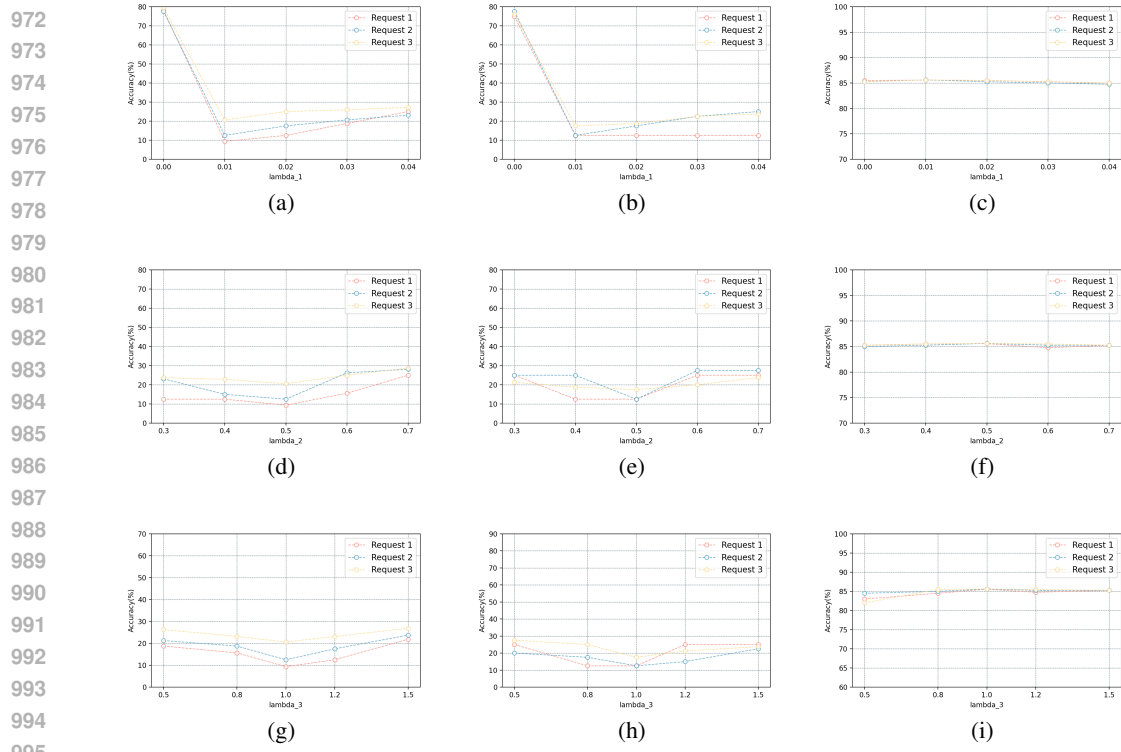


Figure 8: Experimental results on the TOFU dataset. The left column shows the results of S.U., the middle column shows the results of D.U., and the right column shows the results of R.D.. (a) (b) (c) The result of the hyperparameter λ_1 . (d) (e) (f) The result of the hyperparameter λ_2 (S.U.). (g) (h) (i) The result of the hyperparameter λ_3 (S.U.).

1000
1001
1002
1003
1004
1005
1006
1007
1008
1009
1010
1011
1012
1013
1014
1015
1016
1017
1018
1019
1020
1021
1022
1023
1024
1025